Determination of the mass, width, and ($\Sigma\pi/\Lambda\pi$) branching ratio of the $\Sigma(1381)$ baryon*

S. R. Borenstein,† G. R. Kalbfleisch, R. C. Strand, and V. VanderBurg‡
Brookhaven National Laboratory, Upton, New York 11973

J. W. Chapman
Randall Laboratory, University of Michigan, Ann Arbor, Michigan 48104
(Received 21 February 1974)

The mass, width, and ($\Sigma\pi/\Lambda\pi$) branching ratio of the Y_1^* or $\Sigma(1381)$ are reported from a large-statistics sample for which systematic effects are included. The mass values for Y_1^{*+}, Y_1^{*-}, and Y_1^{*0} are found to be 1381 ± 1 MeV, 1383 ± 2 MeV, and 1380 ± 2 MeV, respectively; an average width of 34 ± 2 MeV is found. The $\Sigma\pi$ branching fraction is found to be 0.17 ± 0.04. Good agreement between the latest experimental data for the $J^P = 3/2^+$ decimet and the expectations of SU_3 is obtained by using equal spacing in mass squared and by using the average of the cube of the decay momenta in comparing the partial widths.

I. INTRODUCTION

The $\Sigma(1381)$ or Y_1^* baryon has been extensively studied since its discovery in 1960.[1] However, various properties of the Y_1^* have been only poorly determined, due primarily to disagreements on the values of these parameters in different experiments. The compilation by the Particle Data Group[2] of the mass, width and branching ratios of the $\Sigma(1381)$ is based on about 3500 Y_1^{*+} and about 3500 Y_1^{*-} events; the major fraction of these events (2800 events each of Y_1^{*+} and Y_1^{*-}) come from three experiments: those of Huwe,[3] Armenteros *et al.*,[4] and Siegel.[5] Another 2200 Y_1^* events have been reported by three other experiments: those of Aguilar-Benitez *et al.*,[6] Thomas *et al.*,[7] and Baltay *et al.*[8] The observed mass values for the Y_1^{*-} and the widths of both the Y_1^{*+} and Y_1^{*-} are in poor agreement.[2] The $\Sigma\pi/\Lambda\pi$ branching ratio has been only moderately well determined, with some disagreement among the values, and is based on the observation of about 600 $Y_1^* \to \Sigma\pi$ events.[2,6,7]

We report a determination of the mass and width of the Y_1^{*+} and Y_1^{*-}, as well as the Y_1^{*0}, and of the branching ratio $R = [\Sigma(1381) \to \Sigma\pi]/[\Sigma(1381) \to \Lambda\pi]$ based on about 7000 $Y_1^{*+} \to \Lambda\pi^+$, 2500 $Y_1^{*-} \to \Lambda\pi^-$, 3000 $Y_1^{*0} \to \Lambda\pi^0$, and 240 $Y_1^{*+} \to \Sigma^0\pi^+$.

II. THE DATA SAMPLE

The new results reported here were obtained from about 1.1 million pictures of 2.18-GeV/c K^- taken with the BNL 31-in. liquid hydrogen bubble chamber between 1968 and 1971. The details of the exposure are given elsewhere.[9] Data from the following three reactions were used:

$$K^- + p \to \Lambda\pi^+\pi^- \quad (9100 \text{ events}), \tag{1}$$

$$K^- + p \to \Sigma^0\pi^+\pi^- \quad (3700 \text{ events}), \tag{2}$$

and

$$K^- + p \to \Lambda\pi^+\pi^-\pi^0 \quad (18\,000 \text{ events}). \tag{3}$$

An unbiased pure sample of events was obtained by applying several cuts to the data. The scanning criteria for the events demanded a low momentum transfer $\Delta_{p,\Lambda}{}^2 \equiv -t$ from the target proton to the Λ. This Δ^2 distribution is unbiased for $\Delta_{p,\Lambda}{}^2 \lesssim 1$ GeV^2. In order to have an essentially unbiased sample of events, the data were cut on the momentum transfer from the target proton to the $\Sigma(1381)$, $\Delta_{p,\Sigma}{}^2 \leq 0.7$ GeV^2 for reactions (1) and (2). In addition, no events with a loss of constraints at the production or Λ decay vertices were used, in order to eliminate poorly measured events. This removes the necessity of correcting for the inability to obtain kinematic fits for certain reaction classes when a momentum or angle measurement on some track has been lost. Thus, the total number of constraints was required to be greater than or equal to 7, 5, and 4 for reactions (1), (2), and (3), respectively. These general cuts were applied to all three reactions. Additional cuts are imposed as required in some of the subsequent analyses.

III. MASS AND WIDTH DETERMINATION

All events fitting reaction (1) were taken to be examples of that reaction, since fits ambiguous with reactions (2) or (3) are generally truly examples of reaction (1). This is due to the relatively large cross section of reaction (1) and the highly constrained kinematics of these events. Events not fitting reactions (1) or (2) but fitting reaction (3) were taken to be examples of reaction (3). The $\Lambda\pi$ mass distributions of the events from

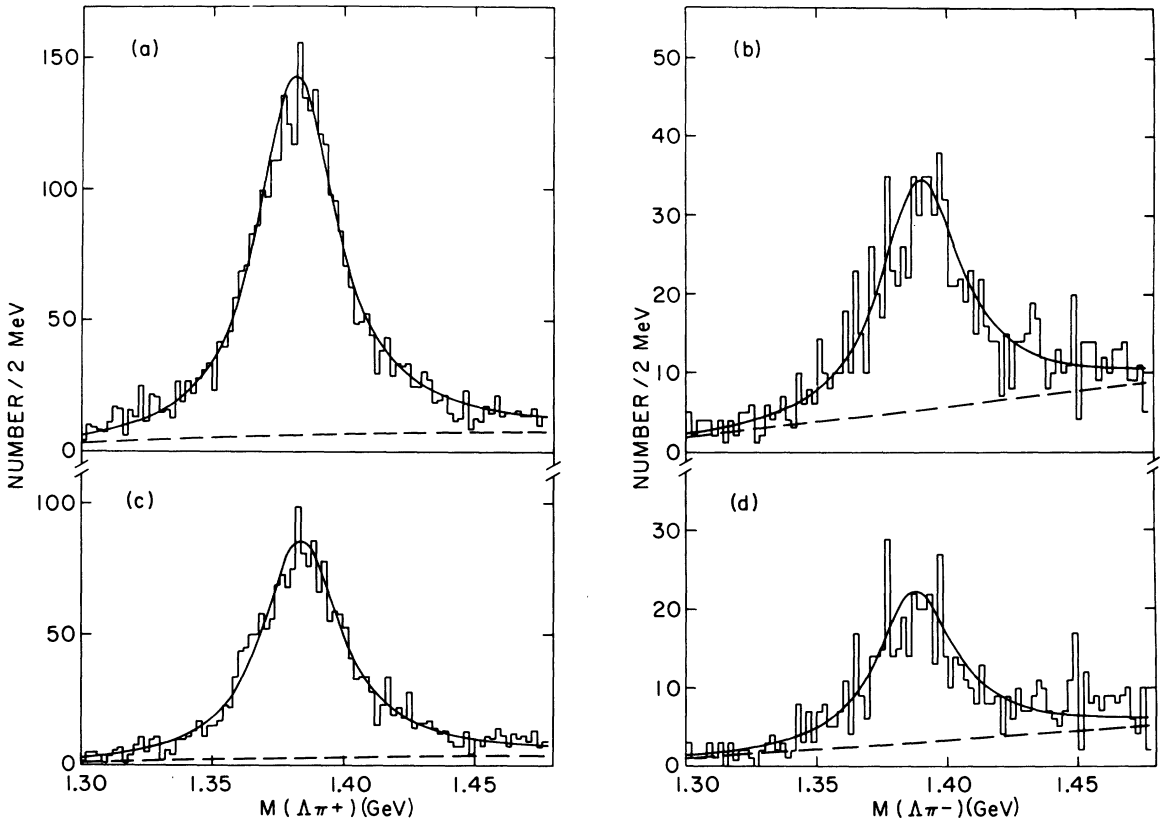

FIG. 1. (a) The $\Lambda\pi^+$ mass distribution and (b) the $\Lambda\pi^-$ mass distribution of the events from the final state $\Lambda\pi^+\pi^-$; (c) and (d) the same as (a) and (b) but with events excluded if $M(\pi^+\pi^-)$ falls in the ρ band, 660–860 MeV; the solid curve and the dashed background curve are the result of the fitting procedure described in the text.

reaction (1) are shown in Fig. 1 and those from reaction (3) are shown in Fig. 2 for mass values from 1.28 to 1.48 GeV. Reaction (1) has a strong contribution from $\Lambda\rho^0(765)$; the $\Lambda\pi$ mass distributions from reaction (1), excluding those events containing a ρ^0, $0.66\ \text{GeV} < M(\pi^+\pi^-) < 0.86\ \text{GeV}$, are also shown in Fig. 1.

The data in Figs. 1 and 2 were fitted to a Breit-Wigner curve with an energy-independent width (called "s-wave" Breit-Wigner in this paper) convoluted with a resolution function and added to a suitable convex background. This fitting procedure is similar to the one that was used to obtain the mass and width of the $\Xi^*(1531)$.[10] The fitted solid curves are drawn on the data in Figs. 1 and 2; the background distributions are drawn as dashed curves. The mass and width values obtained from these fits are summarized in Table I. The mass of $\Sigma^\pm(1381)$ in reaction (1) depends on the ρ^0 cut. The mass values of $\Sigma^-(1381)$ differ in reactions (1) and (3). Also the $\Sigma^0(1381)$ width does not quite agree with the $\Sigma^\pm(1381)$ width. In order to evaluate systematic effects, additional fits to the data were tried as shown in Table II. The dependence of the mass and width values upon the Breit-Wigner parametrization was determined by fitting the $\Sigma^+(1381)$ data, without ρ^0 cut, to various additional forms. The s-wave parametrization given above is labeled (*i*). The others are (*ii*) $(p^*)^2 \times$(s-wave Breit-Wigner), where p^* is the mass-dependent momentum of the decay pion in the $\Sigma(1381)$ rest frame, (*iii*) the Jackson p-wave form[11] with an energy-dependent width, and (*iv*) the Lichtenberg form,[12] where the energy dependence of the width has been separated into a "background" phase shift. Form (*iv*) is close to form (*i*) for the $Y_1^* \to \Lambda\pi$ decay. Forms (*ii*) and (*iii*) shift the mass and width values.[13] In addition, the form (*iii*) does not fit the data of Fig. 1(a) over the range shown; however, a more acceptable fit could be obtained by a more extreme choice of the background, say peaked at low masses, or over a limited mass region near the center of the peak. Since the other forms fit adequately, this possibility was not pursued. The data from reaction (2) are discussed below (Sec. IV) but the fitted mass value, with width fixed, is given here for comparison; note that a larger mass value is obtained for this decay

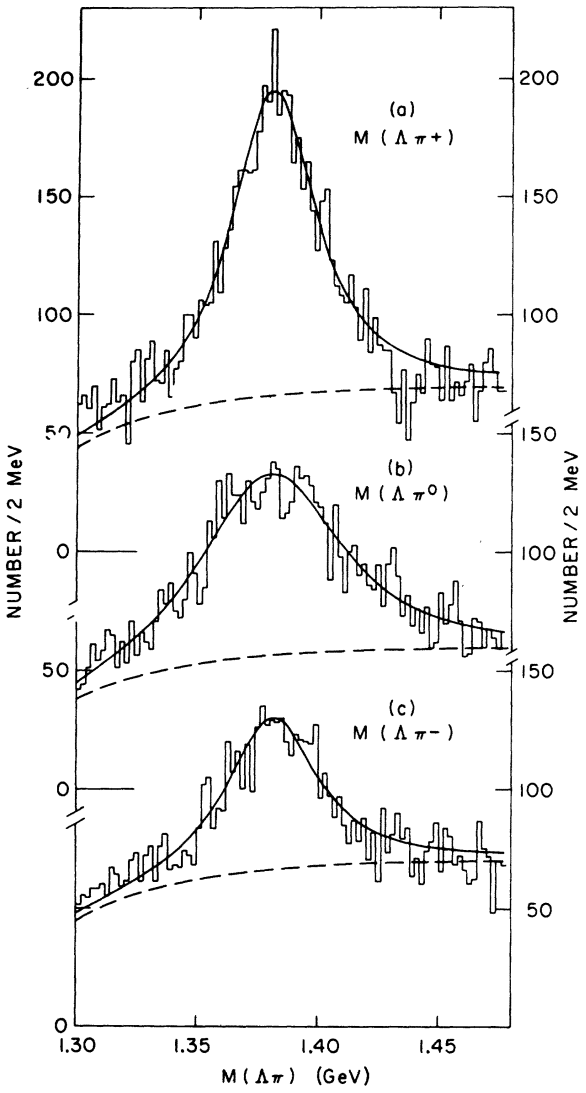

FIG. 2. (a) The $\Lambda\pi^+$ mass distribution, (b) the $\Lambda\pi^0$ mass distribution, and (c) the $\Lambda\pi^-$ mass distribution of the events from the final state $\Lambda\pi^+\pi^-\pi^0$; the solid curve and the dashed background curve are the result of the fitting procedure described in the text.

mode. Since the mass values of the $\Sigma^-(1381)$ obtained from the data of reactions (1) and (3) disagree, fits to the average mass $\overline{M}=1383$ MeV were made (the width and the background were allowed to change). Apart from the relatively poor fit to the data of Fig. 1(b), the hypothesis of $\overline{M}=1383$ MeV is satisfied. A fit constraining the $\Sigma^0(1381)$ width at the over-all average value $\overline{\Gamma}=34\pm1$ MeV was made; a satisfactory fit is obtained. In addition, cuts were made to determine if the presence of the large amount of $Y_1^{*+}(1381)$ and $\omega(783)$ in reaction (3) was responsible for the "large" width; the values of the widths from these fits agree with those given in Table I without such cuts.

We conclude that systematic effects in this experiment, due to some unknown physics effect or instrumental bias, influence the mass and width determination of the Y_1^*. Presumably systematic effects are present in other previously reported experiments and account for the relatively poor agreement in the reported mass and width values of the Y_1^*.

We take the corrected average value of 1381 ± 1 MeV as the mass of Y_1^{*+}, as shown in Table I. Also, we take 1383 ± 2 MeV, the average of the values from the data of Figs. 1(d) and 2(b), as the best estimate of the mass of Y_1^{*-}. And we take the value of 1380 ± 2 MeV as the mass of Y_1^{*0} from the fit shown in Table II with Γ fixed at 34 MeV. The errors allow for the systematic deviations observed in Tables I and II. The widths found for Y_1^{*+}, Y_1^{*-}, and Y_1^{*0} of 34 MeV, 33–38 MeV, and 53 ± 8 MeV, respectively (Table I), are all consistent with a weighted average of 34 ± 1 MeV. We take the width to be 34 ± 2 MeV, where the increased error allows for systematics. We note that the mass values of all three charge states are also consistent with the Y_1^{*+} mass value of 1381 ± 1 MeV.

These values are to be compared with the Particle Data Group[2] values of $M,\Gamma(Y_1^{*+})=1383\pm1$ MeV, 36 ± 3 MeV and $M,\Gamma(Y_1^{*-})=1386\pm2$ MeV, 36 ± 6 MeV, with the values $M,\Gamma(Y_1^{*0})=1385\pm2$ MeV, 39 ± 6 MeV and $M,\Gamma(Y_1^{*-})=1387\pm1.3$ MeV, 48 ± 4 MeV of Thomas *et al.*,[7] and with the $\Gamma(Y_1^{*+})=38\pm3$ MeV and $\Gamma(Y_1^{*-})=52\pm3$ MeV of Baltay and Habibi.[8] We believe our results present improved values of these parameters; we have included estimates of systematic shifts and systematic errors and shown the effect of $\Lambda\rho^0$ events on $M(Y_1^{*\pm})$. Most previous analyses have given only the statistical error on the parameters and have given little justification of the correctness of the central values of these parameters. Disagreements between our values and those of other experiments should be attributed to such systematics, we believe.

IV. BRANCHING RATIO

The branching-ratio determination has been made on the basis of channels (1) and (2). The events in these two channels fall into three categories: (a) unique fit to $\Lambda\pi^+\pi^-$, (b) unique fit to $\Sigma^0\pi^+\pi^-$, (c) ambiguous fit.

On the basis of the data we present, we conclude that categories (a) and (c) are almost entirely $\Lambda\pi^+\pi^-$. The problem that remains is the disposition of events in category (b). A reasonable fraction of the events which fit only $\Sigma\pi\pi$ final states are really $\Lambda\pi^+\pi^-$ which fail to fit. In Fig. 3(a), we show

TABLE I. Mass M and width Γ values for $\Sigma(1381)$ using energy-independent width (so-called s-wave Breit-Wigner parametrization).

Decay mode	Final state	Data of Fig.	Γ_R (MeV)[a]	Fitted mass (MeV)	Corrected mass[b]	Width (MeV)	No. of $\Sigma(1381)$	Confidence level
$\Lambda\pi^+$	$\Lambda\pi^+\pi^-$	1(a)	6.5	1380.9 ± 0.4		34 ± 1.4	3360 ± 99	0.04
	$\Lambda\pi^+\pi^-$ with ρ cut[c]	1(c)	6.5	1383.0 ± 0.6	1381 ± 1	34 ± 1.8	2030	0.48
	$\Lambda\pi^+\pi^-\pi^0$	2(a)	13	1380.4 ± 0.7		34 ± 2.7	3486	0.01
$\Lambda\pi^-$	$\Lambda\pi^+\pi^-$	1(b)	6.5	1388.0 ± 1.1	...	35 ± 4	743	0.02
	$\Lambda\pi^+\pi^-$ with ρ cut[c]	1(d)	6.5	1386.4 ± 1.2	1383 ± 2	33 ± 4	468	0.02
	$\Lambda\pi^+\pi^-\pi^0$	2(b)	13	1380.6 ± 0.9		38 ± 5	1835	0.18
$\Lambda\pi^0$	$\Lambda\pi^+\pi^-\pi^0$	2(c)	20	1380 ± 2	(note d)	53 ± 8	3100	0.50

[a] Γ_R is FWHM (full width at half maximum) resolution; $\Gamma_R = \Gamma_c f^{-1}$, where f is a scale factor and Γ_c is calculated from fitted errors (see Ref. 10).
[b] Correction corresponds to a subtraction of 0.6 ± 0.3 MeV (see Ref. 10).
[c] Events with $0.66 < M(\pi^+\pi^-) < 0.86$ GeV excluded.
[d] See Table II, $\Lambda\pi^0$, $\Gamma = 34$ MeV fixed.

the missing mass of the hyperon, MM_Y, in the reaction hypothesis

$$K^- + p \rightarrow \pi^+\pi^- + (MM_Y) \quad (4)$$

for events fitting reactions (1) or (2). The $\Sigma^0(1192)$ is seen as a bulge on the high-mass side of the Λ peak, as indicated by the arrows. In order to see the Σ^0 more clearly, we examine fits to the reactions

$$K^- + p \rightarrow \Lambda\pi^+\pi^-\gamma \quad (5)$$

and

$$K^- + p \rightarrow \Lambda\pi^+\pi^- MM\,, \quad (6)$$

where MM represents the missing mass. Most of the events fitting reactions (1) or (2) fit hypothesis (5) also; some events with a MM^2 in hypothesis (6) near or below zero and which are examples of reaction (1) do not fit reaction (5). Of the events fitting reactions (1) and (2), better than 99% have a fit to reaction (5) or (6). In Fig. 3(b), we show the $M(\Lambda\gamma)$ distribution from reaction (5) or the

TABLE II. Mass and width values from various additional fits. The different Breit-Wigner parametrizations used are (*i*) s-wave, (*ii*) "p^2" times s-wave, (*iii*) Jackson p-wave form, and (*iv*) Lichtenberg p-wave form (see text). The background was free to be adjusted by the fit.

$\Sigma(1381)$ Decay mode	Final state	Data of Fig.	Special conditions	Parametrization	M_{corr} (MeV)[a]	Γ (MeV)	Confidence level
$\Lambda\pi^+$	$\Lambda\pi^+\pi^-$	1(a)	Different Breit-Wigner parametrizations	(*ii*)	1378.8 ± 0.6	31.4 ± 1.2	0.006
				(*iii*)	1380.7 ± 0.6	31.6 ± 1.3	0[b]
				(*iv*)	1381 (fixed)	34 (fixed)	0.03
$\Sigma^0\pi^+$	$\Sigma^0\pi^+\pi^-$	5(b)	Γ fixed	(*i*)	1389 ± 2.5	36 (fixed)	0.30
$\Lambda\pi^-$	$\Lambda\pi^+\pi^-$	1(b)				36 ± 4	0.001
	$\Lambda\pi^+\pi^-$ with ρ cut	1(d)	M fixed	(*i*)	1383 (fixed)	33 ± 4	0.02
	$\Lambda\pi^+\pi^-\pi^0$	2(b)				39 ± 5	0.18
$\Lambda\pi^0$	$\Lambda\pi^+\pi^-\pi^0$	2(c)	Γ fixed		1380 ± 1.3[d]	34 (fixed)	0.24
			Data of Fig. 2(c) with Y^{*+} removed[c]	(*i*)	1381 ± 2	56 ± 8	0.63
			Data of Fig. 2(c) with Y^{*+} and $\omega(783)$ removed[c]		1380 ± 2	50 ± 8	0.14

[a] The 0.6 ± 0.3 MeV systematic correction has already been included.
[b] χ^2 is 50 greater than the best fit in Table I, which has a χ^2 of 130 for 95 degrees of freedom.
[c] $0.75 < M(\pi^+\pi^-\pi^0) < 0.82$ GeV and $1.35 < M(\Lambda\pi^+) < 1.42$ GeV.
[d] This is taken to be the "best" value of $M(Y_1^{*0})$.

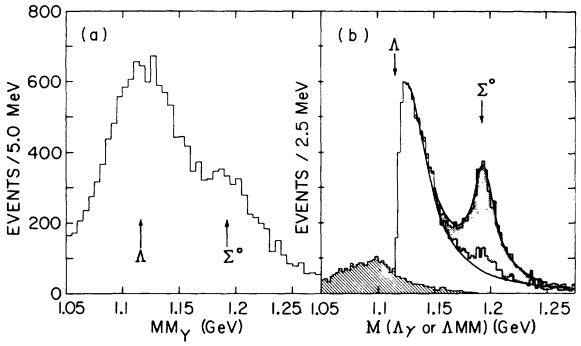

FIG. 3. (a) The missing mass of the hyperon (MM_Y) in the reaction $K^-p \to \pi^+\pi^- MM_Y$. (b) The mass distribution $M(\Lambda\gamma)$ [or $M(\Lambda MM)$] from the final state $\Lambda\pi^+\pi^-\gamma$ (or $\Lambda\pi^+\pi^-MM$) for events fitting $K^-p \to \Lambda\pi^+\pi^-$ or $\Sigma^0\pi^+\pi^-$. The unique Σ^0 events are shown shaded. The $\Lambda\pi^+\pi^-$ events that do not fit $\Lambda\pi^+\pi^-\gamma$ are taken as $\Lambda\pi^+\pi^-MM$ and are shown cross hatched (see text).

$M(\Lambda MM)$ distribution from reaction (6) for events fitting reactions (1) or (2); the $M(\Lambda MM)$ distribution is shown cross-hatched in Fig. 3(b). Those events having a unique Σ^0 interpretation, reaction (2), category (b), are shown shaded in Fig. 3(b). We see a very clear Σ^0 peak. A fit to the $M(\Lambda\gamma$ or $\Lambda MM)$ distribution of a Σ^0 peak plus a background has been made; the upper curve represents such a fit, with the lower curve representing the best estimate of the background. We see that the unique Σ^0 comprise most of the events of reaction (2); however, there is a Σ^0 bump above the background curve in the unshaded part of Fig. 3(b). From the fit, the unique Σ^0 events, with

$$1.178 < M(\Lambda\gamma) < 1.208 \text{ GeV},$$

comprise a fraction of approximately 0.6 of all events of reaction (2).

In order to look for evidence of the decay mode $Y^{*+} \to \Sigma^0\pi^+$, we plot in Figs. 4(a)–4(h) the $M(\Lambda\pi^+)$ distributions of all events fitting reaction (1) subdivided into 15-MeV intervals of $M(\Lambda\gamma$ or $\Lambda MM)$ from hypotheses (5) or (6). A clear $Y_1^{*+} \to \Lambda\pi^+$ signal is seen in all plots 4(a)–4(h) and supports the contention, made above, that all events fitting reaction (1) are indeed examples of that reaction. In Figs. 4(a′)–4(h′), we plot the $M(\Sigma^0\pi^+)$ distributions of the unique Σ^0 events of reaction (2). We see $Y^{*+} \to \Lambda\pi^+$ as a misidentified bump at approximately 1.46 GeV more or less clearly in all of Figs. 4(a′)–4(h′). We see in addition a bump at 1.39 GeV in Figs. 4(d′), 4(e′), and 4(f′), corresponding to the $M(\Lambda\gamma$ or $\Lambda MM)$ regions near the Σ^0 mass. This constitutes clear evidence for the decay $Y_1^{*+} \to \Sigma^0\pi^+$. In order to determine the $\Sigma\pi/\Lambda\pi$ branching ratio, we will confine ourselves to

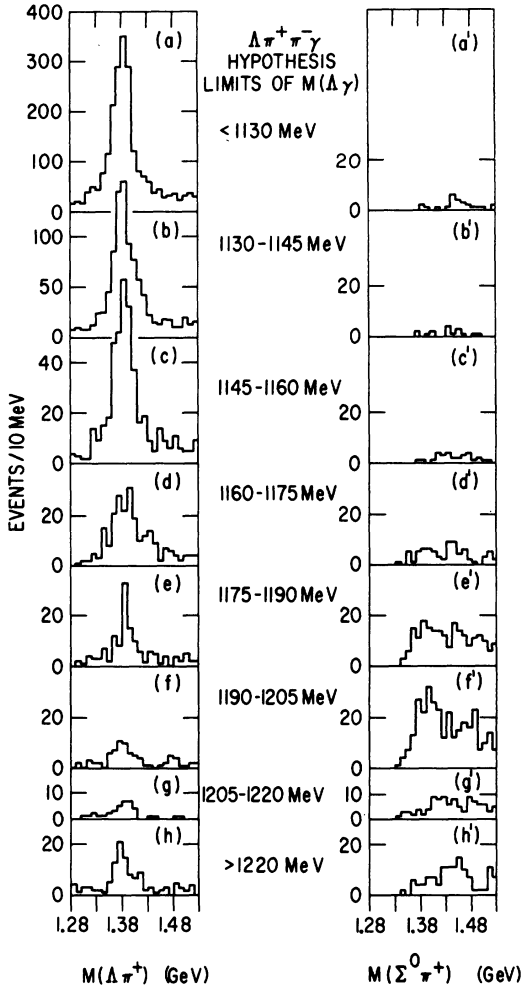

FIG. 4. (a)–(h) The $\Lambda\pi^+$ mass spectrum from the final state $\Lambda\pi^+\pi^-$, and (a′)–(h′) the $\Sigma^0\pi^+$ mass spectrum from the unique $\Sigma^0\pi^+\pi^-$ events as a function of $M(\Lambda\gamma)$. Each plot corresponds to a ≥15-MeV-wide region of the ($\Lambda\gamma$ or ΛMM) mass computed by interpreting these events as $\Lambda\pi^+\pi^-\gamma$ or $\Lambda\pi^+\pi^-MM$ (see text).

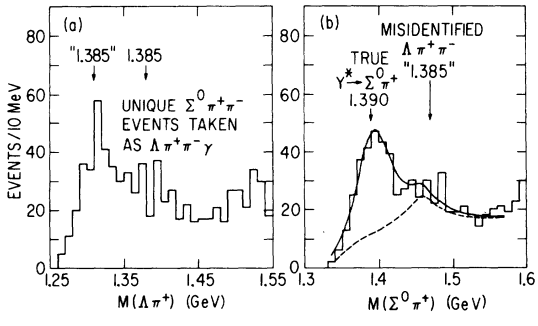

FIG. 5. (a) The $\Lambda\pi^+$ mass spectrum from the unique $\Sigma^0\pi^+\pi^-$ events reinterpreted as $\Lambda\pi^+\pi^-\gamma$; (b) The $\Sigma^0\pi^+$ mass spectrum from unique $\Sigma^0\pi^+\pi^-$ events. This spectrum is approximately the sum of histograms 4(e′) and 4(f′) (see text).

unique Σ^0 events, reaction (2), category (b), which have $1.178 < M(\Lambda\gamma$ or ΛMM$) < 1.208$ GeV, and correct for losses due to these selections. The mass distribution $M(\Sigma^0\pi^+)$ for these unique Σ^0 events is shown in Fig. 5(b); the mass distribution $M(\Lambda\pi^+)$ for these same events, deleting the γ ray by using the fit to reaction (5), are shown in Fig. 5(a). Comparison of Figs. 5(a) and 5(b) shows that the 1.46-GeV $\Sigma^0\pi^+$ "peak" corresponds to misidentified $Y_1^{*+} \to \Lambda\pi^+$ at 1.385 GeV and shows that the 1.39-GeV $\Sigma^0\pi^+$ peak moves down in the $\Lambda\pi^+$ plot. [A scatter-plot of $M(\Lambda\pi^+)$ vs $M(\Sigma^0\pi^+)$ (not shown) shows correspondence on an event-by-event basis.] The data of Fig. 5(b) were then fitted with a $Y_1^{*+} \to \Sigma^0\pi^+$ Breit-Wigner curve of fixed mass and width (M, Γ = 1.389, 0.036 GeV) convoluted with a resolution function of $\Gamma = 20$ MeV FWHM (full width at half maximum) plus a misidentified $\Sigma^+(1381)$ as a Breit-Wigner curve with $(M, \Gamma) = (1.460, 0.055$ GeV) and a background. Various parametrizations of the background can be chosen, which increase or decrease the number of $Y_1^{*+} \to \Sigma^0\pi^+$ events; this variation has been treated as a systematic uncertainty in the number of observed $Y_1^{*+} \to \Sigma^0\pi^+$ decays. We find the number of unique Σ^0 events having $1.178 < M(\Lambda\gamma$ or ΛMM$) < 1.208$ GeV to be 240 ± 60 events, including the background variation uncertainty of ± 50 added in quadrature. In order to correct for the loss of $\Sigma^0\pi^+\pi^-$ events due to these selections, we plot in Fig. 6, as in Fig. 3(b), the mass distribution $M(\Lambda\gamma)$ for the events of reaction (1) or (2) where $M(\Lambda\pi^+$ or $\Sigma^0\pi^+) < 1.480$ GeV. This is done since the loss correction depends on the mass resolution of the Σ^0 signal; the $M(\Lambda\gamma)$ resolution is better for events with $M(\Sigma^0\pi^+)$ near the Y_1^* mass. A fit of a Σ^0 peak plus background is again made and is shown as the curves on the data of Fig. 6. From this fit, the unique $Y_1^{*+} \to \Sigma^0\pi^+$ events of reaction (2) under the stated selections comprise a fraction 0.70 ± 0.04 of all such events. The 1460-MeV misidentified $Y_1^{*+} \to \Lambda\pi^+$ events shown in Fig. 6 are about 4% of the number found from the data of Fig. 1(a). There is no correction to be made for events which only fit hypothesis (6) and for which the $MM^2 < 0$, since events truly belonging to reactions (1) and (2) are equally lost [the number of events making a "fit" to hypothesis (6) only is about 5% of the number of events found to fit reactions (1) and (2)]. Thus the $(\Sigma^0\pi^+/\Lambda\pi^+)$ branching ratio of the $\Sigma(1381)$ is

$$R_1 = \frac{Y_1^{*+} \to \Sigma^0\pi^+}{Y_1^* \to \Lambda\pi^+} = \frac{(240 \pm 60)/(0.70 \pm 0.04)}{(1.04 \pm 0.01)(3360 \pm 99)} = 0.098 \pm 0.025 .$$

This is our primary branching-ratio result. The other decay mode $Y_1^{*+} \to \Sigma^+\pi^0$ should yield an equal number of events ignoring barrier and phase-space effects. However, taking these effects into account, the number of $Y_1^{*+} \to \Sigma^+\pi^0$ events should be 1.1 ± 0.03 times the number of $Y_1^{*+} \to \Sigma^0\pi^+$ (see Sec. V). Thus the $(\Sigma\pi/\Lambda\pi)$ branching ratio is

$$R_2 = \frac{Y_1^{*+} \to (\Sigma\pi)^+}{Y_1^* \to (\Lambda\pi)^+} = 2.1\,R_1 = 0.21 \pm 0.05 ,$$

or the $\Sigma\pi$ branching fraction is

$$R_3 = \frac{Y_1^* \to \Sigma\pi}{Y_1^* \to \Lambda\pi \text{ or } \Sigma\pi} = \frac{2.1N(\Sigma^0\pi^+)}{N(\Lambda\pi^+) + 2.1N(\Sigma^0\pi^+)} = 0.17 \pm 0.04 .$$

These values of R_1, R_2, R_3 are all higher than those found in previous determinations. Our value of R_1 is in poor agreement with the result of Huwe of 0.045 ± 0.005,[3] based on about 300 events. Our value of R_2 is in reasonable agreement with the low-statistics results of Pan and Forman[14] of 0.13 ± 0.04, of Colley *et al.*[15] of 0.13 ± 0.04, of Aguilar-Benitez *et al.*[6] of 0.16 ± 0.07, and of Thomas *et al.*[7] of 0.10 ± 0.05. Finally, our value of R_3 is in good agreement with the result of Armenteros *et al.*[4] of 0.14 ± 0.03, based on about 170 events. No systematic errors are given for the earlier results.

We believe that the detailed procedure presented

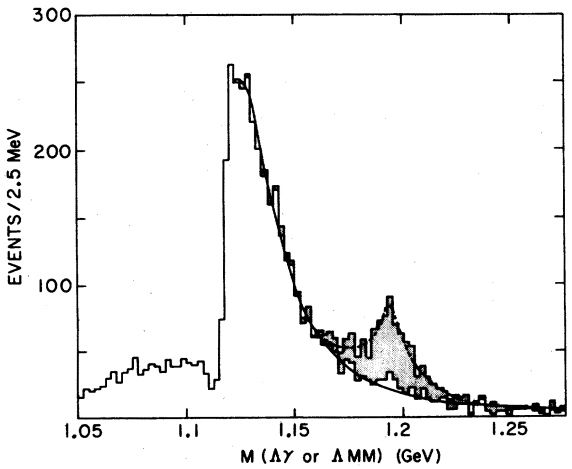

FIG. 6. The mass distribution $M(\Lambda\gamma$ or ΛMM$)$ as in Fig. 3(b), for $\Lambda(\Sigma^0)\pi^+\pi^-$ events having $M(\Lambda\pi^+$ or $\Sigma^0\pi^+) < 1.48$ GeV. The unique Σ^0 are again shown shaded.

here, which accounts for all events and takes account of systematic effects due to background variations, etc., in the relationship of reactions (1) and (2) to hypotheses (5) and (6), gives the best determination of the $\Sigma(1381)$ branching ratio. We note that the various theoretical estimates of this branching ratio (R_3) based on SU_3 are typically 15% (see Sec. V below).

A final test that the 1.39-GeV $\Sigma^0\pi^+$ signal of Fig. 5(b) is indeed a decay mode of the $\Sigma(1381)$ is given in Fig. 7. London *et al.*[16] observed a characteristic $(1+3\cos^2\theta)$ production-decay correlation distribution for the $Y_1^{*+}\to\Lambda\pi^+$ characteristic of a peripherally produced $J=\frac{3}{2}$ state. The angle $\theta=\hat{\pi}^+\cdot\hat{N}$, where $\hat{\pi}^+$ is the direction of decay pions' momentum in Y_1^* rest frame and $\hat{N}$ is the unit normal to the production plane, $\vec{N}=\vec{K}_{in}^-\times\vec{Y}_{out}^*$. The $\hat{\pi}^+\cdot\hat{N}$ distribution for our $Y_1^{*+}\to\Lambda\pi^+$ events of reaction (1), with $1.347<M(\Lambda\pi^+)<1.419$ GeV, is shown in Fig. 7(a) and is compatible with a $(1+3\cos^2\theta)$ distribution plus a small background.

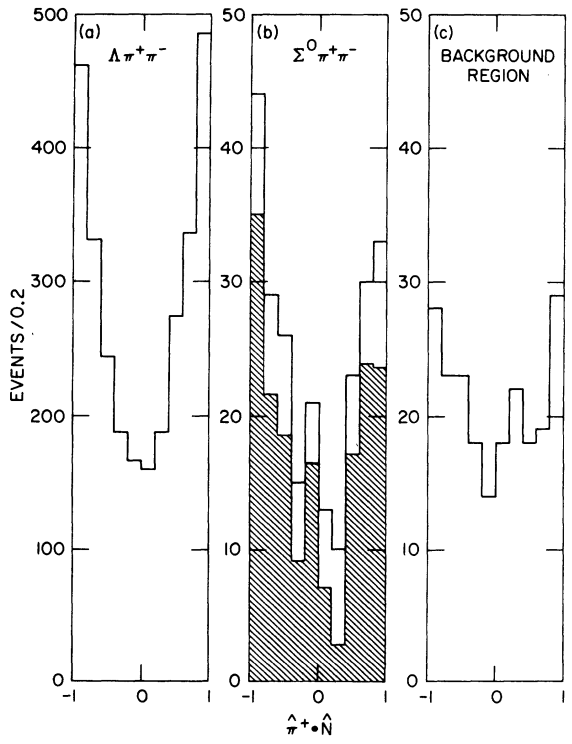

FIG. 7. The cosine of the angle between the decay π^+ meson and the normal $\hat{N}$ to the production plane, in the Y^* rest frame. (a) The $\Lambda\pi^+\pi^-$ final state with the $\Lambda\pi^+$ mass between 1347 and 1419 MeV/c^2. (b) The $\Sigma^0\pi^+\pi^-$ final state with the $\Sigma^0\pi^+$ mass between 1347 and 1419 MeV/c^2. (c) The $\Sigma^0\pi^+\pi^-$ final state with the $\Sigma^0\pi^+$ mass between 1420 and 1500 MeV/c^2 to observe behavior in a background region. The cross-hatched area in (b) corresponds to a background subtraction using the data from (b) and (c).

The $\hat{\pi}^+\cdot\hat{N}$ distribution for $Y_1^{*+}\to\Sigma^0\pi^+$ $[1.347<M(\Sigma^0\pi^+)<1.419$ GeV] is shown in Fig. 7(b) and for a background region of $\Sigma^0\pi^+$ $[1.42<M(\Sigma^0\pi^+)<1.50$ GeV] in Fig. 7(c). The "subtracted" $Y_1^{*+}\to\Sigma^0\pi^+$ distribution is shown cross-hatched in Fig. 7(b) and is reasonably consistent with a $(1+3\cos^2\theta)$ distribution as is required if the $\Sigma^0\pi^+$ events are indeed an alternate decay mode of the $\Sigma(1381)$. We note that the fits, Tables I and II, for the mass and width of the Y_1^{*+} of Fig. 1(a) required a background consistent with that of Fig. 7(a). That such a background is probably incoherent is seen from the forward/backward (F/B) and polar/equatorial (P/E) ratios for the angular distribution in Fig. 7(a) as a function of mass, shown in Table III. The F/B ratio is the number of events with $\cos\theta>0$ relative to the number with $\cos\theta<0$; the P/E ratio is the number of events with $|\cos\theta|>0.6$ relative to the number with $|\cos\theta|<0.6$. In the absence of interference, the F/B ratio is expected to be 1. For a pure $(1+3\cos^2\theta)$ distribution the P/E ratio should be 1.45. The F/B ratios and the P/E ratios over the mass values corresponding to the Y_1^* peak, i.e., $M(\Lambda\pi^+)<1442$ MeV, are all consistent with the average values of 1.04 ± 0.03 and 1.25 ± 0.04, respectively.

V. DISCUSSION

The four different parametrizations of Breit-Wigner amplitudes lead to different values of the mass and width parameters as was seen in Table II. The values deviate more widely for broader resonances. The shifts in mass and width for the four different parametrizations are illustrated for the $\Sigma^+(1381)$ in Table IV, where the value of the mass at the peak of the distribution M_p, the average mass $\bar{M}$ (averaged over plus and minus 3 half-widths), and the resultant full width at half maximum Γ_p are given for the different Breit-Wigner forms. The results are given for both the $\Lambda\pi^+$ and the $\Sigma^0\pi^+$ decay modes. As pointed out above, the $\Sigma^0\pi^+$ data peaks higher (1389 ± 2.5 MeV) than does the $\Lambda\pi^+$ data. This also favors the Lichtenberg[12] form (*iv*) over the Jackson[11] form (*iii*). Better phenomenological and/or theoretical treat-

TABLE III. F/B and P/E ratios for Y_1^{*+} (see text).

Region of $M(\Lambda\pi^+)$	F/B	P/E
(1262 MeV, 1322 MeV)	0.91 ± 0.12	1.18 ± 0.16
(1322 MeV, 1362 MeV)	1.01 ± 0.08	1.37 ± 0.12
(1362 MeV, 1382 MeV)	1.05 ± 0.07	1.31 ± 0.08
(1382 MeV, 1402 MeV)	1.08 ± 0.06	1.31 ± 0.08
(1402 MeV, 1442 MeV)	0.91 ± 0.07	1.27 ± 0.10
(1442 MeV, 1502 MeV)	1.20 ± 0.12	0.88 ± 0.09
(> 1502 MeV)	1.05 ± 0.03	0.63 ± 0.02

TABLE IV. Mass and width shifts for the $\Sigma^+(1381)$ from different Breit-Wigner parametrizations: (*i*) *s*-wave, (*ii*) "p^2" times *s*-wave, (*iii*) Jackson *p*-wave form, and (*iv*) Lichtenberg *p*-wave form (see text). The nominal mass and width parameters are (M,Γ) = (1381 MeV, 34 MeV). Given are the mass value at the peak of the distribution M_p, the average value of the mass $\bar{M}$ (averaged over plus and minus three half-widths), and the actual full width at half-maximum Γ_p.

	Parametrization	M_p (MeV)	$\bar{M}$ (MeV)	Γ_p (MeV)
$\Sigma^+(1381)\to\Lambda\pi^+$	(*i*)	1381.8	1383.0	34
	(*ii*)	1383.3	1386.8	35
	(*iii*)	1379.2	1383.4	33
	(*iv*)	1381.8	1382.8	33
$\Sigma^+(1381)\to\Sigma^0\pi^+$	(*i*)	1382.8	1386.2	34
	(*ii*)	1385.8	1393.5	40
	(*iii*)	1377.3	1386.0	27
	(*iv*)	1386.3	1393.9	40

ments of the parametrization of resonant amplitudes appears to be needed.

The $J^P=\frac{3}{2}^+$ decimet, Δ, Y_1^*, $\Xi^*(1531)$, and Ω^-, should have the simplest SU_3 structure. The masses are expected to obey the equal mass-spacing rule (in lowest order) and the widths should all be related to one matrix element or coupling constant through "SU_3 Clebsch-Gordan" coefficients. Samios, Goldberg, and Meadows[17] find in their SU_3 review that both of these expectations are nearly satisfied. However, Baltay *et al.*[8] find that the equal mass-spacing rule is violated and that the decay widths are somewhat incompatible. We find that the simple SU_3 expectations are well satisfied under somewhat modified conditions.

For the broad Δ baryon the Breit-Wigner parametrization has been a problem; the Particle Data Group[2] and others[18] have discussed this. The Δ can be characterized by the "peak" mass and width values of 1236 ± 4 MeV and 116 ± 6 MeV, respectively,[2,17] or by the "pole" values, 1211.6 ± 0.7 MeV and 99.0 ± 3.6 MeV, respectively.[2,12]

The mass values of Y_1^{*-} (this experiment) and the recently improved values for Ξ^{*-} (Ref. 2) and Ω^- (Ref. 2) are 1383 ± 2 MeV, 1535.0 ± 0.6 MeV, and 1672.5 ± 0.5 MeV, respectively. The (Ξ^{*-}, Y_1^{*-}) mass difference of 152 ± 2 MeV is *not* equal to the (Ω^-,Ξ^{*-}) mass difference of 137.5 ± 0.8 MeV, as noted by Baltay *et al.*[8] However, note that the mass-squared values of 1.913 ± 0.005, 2.356 ± 0.002, and 2.797 ± 0.002 GeV^2, respectively, have the corresponding differences of 0.443 ± 0.006 GeV^2 and 0.441 ± 0.003 GeV^2. These are equal within errors. Equal mass-squared spacing then predicts the Δ mass squared to be $(1.913\pm0.005)-(0.442\pm0.003)=1.471\pm0.006$ GeV^2; that is, the Δ mass should be 1213 ± 2.5 MeV, which is within one standard deviation of the pole value.[19]

The decay rate formula of Samios, Goldberg, and Meadows[17] is

$$\Gamma_i=\frac{1}{M}|A_{10}|^2\times(\mathrm{SU_3\ factors})\times\left(\frac{p_i^*}{M}\right)^{2l}\frac{p_i^*}{m_i},$$

where Γ_i is the partial decay rate for a given decimet decay mode i, M is an arbitrary mass for dimensional reasons (=1 GeV/c^2), A_{10} is the decimet matrix element, l is the orbital angular momentum, p_i^* is the decay momentum, and m_i is the mass value of decimet member i.[20] We find that good results are obtained using the pole masses m_i and using the value of $(p_i^*)^3$ averaged over the mass distribution for decay mode i. The various Breit-Wigner parametrizations give somewhat differing results. The width predictions for the four forms used before are given in Table V and compared with the experimental data. The *s*-wave form, which is not expected to be correct, is clearly ruled out. The pole value of the Δ width is chosen. Of the *p*-wave forms, the Lichtenberg[12] form (iv) appears to be the best.

VI. CONCLUSIONS

We present new results for the mass, width, and ($\Sigma\pi/\Lambda\pi$) branching ratio of the $\Sigma(1381)$. Systematic shifts in the mass of $Y_1^{*\pm}$ due to $\Lambda\rho^0$ events or background parametrizations preclude a mass-difference measurement in this experiment (and presumably also in all prior experiments); limits, however, can be given, which are

$$-2<M(Y^{*-})-M(Y^{*+})<6\ \mathrm{MeV}$$

[95% confidence level (C.L.)],

and

$$|M(Y^{*0})-M(Y^{*+})|<4\ \mathrm{MeV}\quad(95\%\ \mathrm{C.L.}).$$

The branching fraction

$$R_3=\frac{\Sigma(1381)\to\Sigma\pi}{\Sigma(1381)\to\mathrm{all}}$$

$$=0.17\pm0.04$$

TABLE V. Width predictions from SU_3 for the $J^P = \frac{3}{2}^+$ decimet using four different Breit-Wigner parametrizations: (*i*) *s*-wave, (*ii*) "p^2" times *s*-wave, (*iii*) Jackson *p*-wave form, and (*iv*) Lichtenberg *p*-wave form (see text). The predictions are based on the average value of "p" for (*i*) and of "p^3" for (*ii*), (*iii*), and (*iv*) over plus and minus three half-widths of the Breit-Wigner distribution and are normalized to $\Gamma = 28$ MeV for $\Sigma(1381) \to \Lambda\pi^+$ [see note a].

Decimet member	Decay mode	Partial widths (FWHM) in MeV Parametrization				Experiment
		(*i*)	(*ii*)	(*iii*)	(*iv*)	
Δ^{++} (1211 MeV)[b]	$p\pi^+$	79[c]	153[c]	123[c]	104	99.0 ± 3.6[b,d]
Σ^+ (1381 MeV)	$(\Sigma\pi)^+$	11.8	5.4	4.7	5.7	5.8 ± 1.5[a]
Ξ^{*0} (1531 MeV)	$(\Xi\pi)^0$	17.7	8.4	8.6	8.8	9.1 ± 0.5[d]
Σ^+ (1381 MeV)	$\Sigma^0\pi^+$	5.7	2.5	2.2	2.7	2.8 ± 0.7[a]
	$\Sigma^+\pi^0$	6.1	2.9	2.5	3.0	...

[a] Values from this experiment.
[b] "Pole" values for (M, Γ) of Δ^{++}.
[c] We use $M = 1233$ MeV for the Δ^{++} for parametrizations (*i*), (*ii*), and (*iii*); these predictions should possibly be compared with $\Gamma = 116 \pm 6$ MeV ("peak" value).
[d] See Ref. 2.

is larger than the Particle Data Group average[2] of 0.11 ± 0.04 and is in good agreement with the result of Armenteros *et al.*[4] of 0.14 ± 0.03. Systematic corrections to the branching ratio and contributions to the errors in previous experiments need to be made.

We observe that the SU_3 predictions for the decimet are correct if equal spacing in mass squared of the so-called pole values is used and if the value of $(p^*)^3$ averaged over the mass distribution is used in the rate prediction for the widths. We know of no justification for the use of the pole mass squared. Of the phenomenological treatments for the parametrization of Breit-Wigner amplitudes, the Lichtenberg form[12] appears to be preferable.

ACKNOWLEDGMENTS

We thank Dr. R. I. Louttit, Dr. N. P. Samios, and Professor B. Roe for their support and encouragement.

*Work supported by the U. S. Atomic Energy Commission.
†Present address: Ecole Polytechnique, Paris, France (on leave from York College, City University of New York, Queens, New York).
‡Present address: American Electric Power Service Company, 2 Broadway, New York, New York.

[1] M. Alston *et al.*, Phys. Rev. Lett. 5, 520 (1960).
[2] Particle Data Group, Rev. Mod. Phys. 45, S1 (1973).
[3] D. Huwe, Phys. Rev. 181, 1824 (1969).
[4] R. Armenteros *et al.*, Phys. Lett. 19, 75 (1965).
[5] D. M. Siegel, Ph.D. thesis, UCRL Report No. UCRL-18041 (unpublished) (see Ref. 2).
[6] M. Aguilar-Benitez *et al.*, Phys. Rev. D 6, 29 (1972).
[7] D. W. Thomas *et al.*, Nucl. Phys. B56, 15 (1973).
[8] C. Baltay *et al.*, in *Baryon Resonances—73*, edited by E. C. Fowler (Purdue Univ. Press, Lafayette, Indiana, 1973), p. 387; M. Habibi, Columbia Univ., New York, Ph.D. thesis, 1973 (unpublished).
[9] J. S. Danburg *et al.*, Phys. Rev. D 8, 3744 (1973).
[10] S. R. Borenstein *et al.*, Phys. Rev. D 5, 1559 (1972).
[11] J. D. Jackson, Nuovo Cimento 34, 1644 (1963); this *p*-wave Breit-Wigner form has been used by M. Aguilar-Benitez *et al.* (see Ref. 6), and C. Baltay *et al.* (see Ref. 8).
[12] D. B. Lichtenberg, in *Baryon Resonances—73* (Ref. 8), p. 23; we use his "formation" experiment form of the *p*-wave Breit-Wigner form, that is $(p^*)^{-2}|T|^2$, where T is the transition matrix given in his paper; we use his value of $b_0(\Delta^{++}) = 3.57$ for the Y_1^* also.
[13] Form (*iii*) shifts the M, Γ parameters of the broad Δ^{++} (1211 MeV) state appreciably.
[14] Y. Pan and F. L. Forman, Phys. Rev. Lett. 23, 808 (1969).
[15] D. C. Colley *et al.*, Nucl. Phys. B31, 61 (1971).
[16] G. W. London *et al.*, Phys. Rev. 143, 1034 (1966).
[17] N. P. Samios, M. Goldberg, and B. T. Meadows, Rev. Mod. Phys. 46, 49 (1974).
[18] See, e.g., J. Ball *et al.*, Phys. Rev. Lett. 28, 1143 (1972); also see Ref. 12.
[19] Note that the octet baryons also satisfy a mass-squared formula reasonably well (a 1.3% difference using mass squared *vs* a 0.7% difference using mass, in comparison of the appropriate averages of the neutron and Ξ^0 with Λ and Σ^0).
[20] The decay-rate formula of Baltay *et al.* (Ref. 8) contains another factor which is the mass of the decay baryon m_B^i; note that m_B^i/m_i changes more slowly between different members of the decimet than the m_i^{-1} factor of Samios, Goldberg, and Meadows (Ref. 17).